Does Dark Matter at the Center and in the Halo of the Galaxy Consist of the Same Particles?

Neven Bilić[1] , Faustin Munyaneza, Gary B. Tupper,
and Raoul D. Viollier[2]

Institute of Theoretical Physics and Astrophysics
Department of Physics, University of Cape Town
Private Bag, Rondebosch 7701, South Africa

After a discussion of the properties of degenerate fermion balls, we analyze the orbits of the star S0-1, which has the smallest projected distance to Sgr A*, in the supermassive black hole as well as in the fermion ball scenarios of the Galactic center. It is shown that both scenarios are consistent with the data, as measured during the last six years by Genzel *et al.* and Ghez *et al.*. We then consider a self-gravitating ideal fermion gas at nonzero temperature as a model for the Galactic halo. The Galactic halo of mass $\sim 2\times 10^{12} M_\odot$ enclosed within a radius of $\sim$ 200 kpc implies the existence of a supermassive compact dark object at the Galactic center that is in hydrostatic and thermal equilibrium with the halo. The central object has a maximal mass of $\sim 2.3 \times 10^6 M_\odot$ within a minimal radius of $\sim$ 18 mpc or $\sim$ 21 light-days for fermion masses $\sim$ 15 keV. We thus conclude that both the supermassive compact dark object and the halo could be made of the same weakly interacting $\sim$ 15 keV particle.

PRESENTED AT

COSMO-01
Rovaniemi, Finland,
August 29 – September 4, 2001

[1]Permanent address: Rudjer Bošković Institute, P.O. Box 180, 10002 Zagreb, Croatia
Email: bilic@thphys.irb.hr
[2]Email: viollier@physci.uct.ac.za

1 Introduction

In the past, self-gravitating degenerate neutrino matter has been suggested as a model for quasars, with neutrino masses in the 0.2keV $\lesssim m \lesssim$ 0.5MeV range [1]. Later it was used to describe dark matter in clusters of galaxies and in galactic halos, with neutrino masses in the $1 \lesssim m/\mathrm{eV} \lesssim 25$ range [2]. More recently, supermassive compact dark objects consisting of weakly interacting degenerate fermionic matter, with fermion masses in the $10 \lesssim m/\mathrm{keV} \lesssim 20$ range, have been proposed [3, 4, 5, 6, 7] as an alternative to the supermassive black holes that are believed to reside at the centers of many galaxies. It has been pointed out that such degenerate fermion balls could cover [5] the whole range of the supermassive compact dark objects that have been observed so far with masses ranging from 10^6 to $3\times10^9\,M_\odot$ [8]. Most recently, it has been shown that a weakly interacting dark matter particle in the mass range $1 \lesssim m/\mathrm{keV} \lesssim 5$ could solve the problem of the excessive structure generated on subgalactic scales in N-body and hydrodynamical simulations of structure formation in this Universe [9].

So far the masses of ~ 20 supermassive compact dark objects at the center of galaxies have been measured using various techniques [8]. The most massive compact dark object ever observed is located at the center of M87 in the Virgo cluster, and it has a mass of about $3\times10^9 M_\odot$ [10]. If we identify this object of maximal mass with a degenerate fermion ball at the Oppenheimer-Volkoff (OV) limit [11], i.e., $M_{\mathrm{OV}} = 0.54 M_{\mathrm{Pl}}^3\, m^{-2} g^{-1/2} \simeq 3\times10^9 M_\odot$ [5], where $M_{\mathrm{Pl}} = \sqrt{\hbar c/G}$ denotes the Planck mass, this allows us to fix the fermion mass to $m \simeq 15$ keV for a spin and particle-antiparticle degeneracy factor of $g = 2$. Such a relativistic object would have a radius of $R_{\mathrm{OV}} = 4.45 R_{\mathrm{S}} \simeq 1.5$ light-days (1.19 light-days = 1 mpc), where R_{S} is the Schwarzschild radius of the mass M_{OV}. It would thus be virtually indistinguishable from a black hole of the same mass, as the closest stable orbit around a black hole has a radius of 3 R_{S} anyway.

Near the lower end of the observed mass range is the compact dark object located at the Galactic center [12] with a mass of $M_{\mathrm{c}} \simeq 2.6\times10^6 M_\odot$. Interpreting this object as a degenerate fermion ball consisting of $m \simeq 15$ keV and $g = 2$ fermions, the radius is $R \simeq 21$ light-days $\simeq 7\times10^4 R_{\mathrm{S}}$ [3], R_{S} being the Schwarzschild radius of the mass M_{c}. Such a nonrelativistic object is far from being a black hole. The shallowness of its gravitational potential may be probed by infalling gas and stars orbiting within this fermion ball. A particle at infinity at rest falling towards the fermion ball can merely acquire the escape velocity of ~ 1700 km/s from the center of the fermion ball. Therefore the spectrum of the radiation emitted by the infalling gas will be cut off at high frequencies, as is actually seen in the far infrared spectrum of the enigmatic radio source Sgr A* at the Galactic center [13]. From the observed cut-off at $\sim 10^{13}$ Hz, corresponding to emission at ~ 10 light-days, in a thin accretion disk scenario, one can deduce a lower limit for the radius of $R \gtrsim$ 18 light-days [6]. Similarly, the observed motion of stars within a projected distance of ~ 6 to ~ 50 light-days from Sgr A* [12] yields, apart from the mass, an upper limit for the radius of the fermion ball $R \lesssim$ 22 light-days.

The required weakly interacting fermion of $\sim$ 15 keV mass cannot be an active neutrino, as it would overclose the Universe by orders of magnitude [14]. Moreover, an active neutrino of $\sim$ 15 keV is disfavored by the experimental data on solar and atmospheric neutrinos, as these are most probably oscillating into active neutrinos with small δm^2 [15], and the $\nu_{\rm e}$ mass has been determined to be < 3 eV [16]. However, the $\sim$15 keV fermion could very well be a sterile neutrino, contributing $\Omega_{\rm d} \simeq 0.3$ to the dark matter fraction of the critical density today. Indeed, as has been shown for an initial lepton asymmetry of $\sim 10^{-3}$, a sterile neutrino of mass $\sim$ 10 keV may be resonantly produced in the early Universe with near closure density, i.e. $\Omega_{\rm d} \sim 1$ [17]. The resulting energy spectrum of the sterile neutrinos is cut off for energies larger than the resonance energy, thus mimicking a degenerate fermion gas. As an alternative possibility, the $\sim$ 15 keV sterile neutrino could be replaced by the axino [18] or the gravitino [19, 20] in soft supersymmetry breaking scenarios.

In the recent past, galactic halos have been successfully modeled as a self-gravitating isothermal gas of particles of arbitrary mass, the density of which scales asymptotically as r^{-2}, yielding flat rotation curves [21]. As the supermassive compact dark objects at the galactic centers are well described by a gas of fermions of mass $m \sim 15$ keV at $T = 0$, it is tempting to explore the possibility that one could describe both the supermassive compact dark objects and their galactic halos in a unified way in terms of a fermion gas at finite temperature. We will show in this paper that this is indeed the case, and that the observed dark matter distribution in the Galactic halo is consistent with the existence of a supermassive compact dark object at the center of the Galaxy which has about the right mass and size, and is in thermal and hydrostatic equilibrium with the halo.

2 Dynamics of the Stars Near the Galactic Center

We now would like to compare the predictions of the black hole and fermion ball scenarios of the Galactic center, for the stars with the smallest projected distances to Sgr A*, based on the measurements of their positions during the last six years [7, 12]. The projected orbits of three stars, S0-1 (S1), S0-2 (S2) and S0-4 (S4), show deviations from uniform motion on a straight line during the last six years, and they thus may contain nontrivial information about the potential. For our analysis we have selected the star, S0-1, because its projected distance from Sgr A* in 1995.53, 4.4 mpc or 5.3 light-days, makes it most likely that it could be orbiting within a fermion ball of radius $\sim$ 18 mpc or $\sim$21 light-days. We thus may in principle distinguish between the black hole and fermion ball scenarios for this star.

The dynamics of the stars in the gravitational field of the supermassive compact dark object can be studied solving Newton's equation of motion, taking into account the initial position and velocity vectors at, e.g., $t_0 = 1995.4$ yr, i.e., $\vec{r}(t_0) \equiv (x, y, z)$ and $\dot{\vec{r}}(t_0) \equiv (v_x, v_y, v_z)$. For the fermion ball the source of gravitational field is the mass $\mathcal{M}(r)$ enclosed within a radius r [3, 7] while for the black hole it is $M_c = \mathcal{M}(R_c) = 2.6 \times 10^6 M_\odot$.

The x-axis is chosen in the direction opposite to the right ascension (RA), the y-axis in the direction of the declination, and the z-axis points towards the sun. The black hole and the center of the fermion ball are assumed to be at the position of Sgr A* which is also the origin of the coordinate system at an assumed distance of 8 kpc from the sun.

In Figs. 1 and 2 the right ascension (RA) and declination of S0-1 are plotted as a function of time for various unobservable z's and $v_z = 0$ in 1995.4, for the black hole and fermion ball scenarios. The velocity components $v_x = 340$ km s^{-1} and $v_y = -1190$ km s^{-1} in 1995.4 have been fixed from observations. In the case of a black hole, both RA and declination depend strongly on z in 1995.4, while the z-dependence of these quantities in the fermion ball scenario is rather weak. We conclude that the RA and declination data of S0-1 are well fitted with $|z| \approx 0.25''$ in the black hole scenario, and with $|z| \lesssim 0.1''$ in the fermion ball case ($1'' = 38.8$ mpc $= 46.2$ light-days at 8 kpc). Of course, we can also try to fit the data varying both the unknown radial velocity v_z and the unobservable radial distance z. The results are summarized in Fig. 3, where the $z - v_z$ phase-space of 1995.4, that fits the data, is shown. The small range of acceptable $|z|$ and $|v_z|$ values in the black hole scenario (solid vertical line) reflects the fact that the orbit of S0-1 depend strongly on z. The weak sensitivity of the orbit on z in the fermion ball case is the reason for the much larger $z - v_z$ phase-space fitting the data of S0-1 [12], as shown by the dashed box. The dashed and solid curves describe the just bound orbits in the fermion ball and black hole scenarios, respectively. The star S0-1 is unlikely to be unbound, because in the absence of close encounters with stars of the central cluster, S0-1 would have to fall in with an initial velocity that is inconsistent with the velocity dispersion of the stars at infinity.

Fig. 4 shows some typical projected orbits of S0-1 in the black hole and fermion ball scenarios. The data of S0-1 may be fitted in both scenarios with appropriate choices of v_x, v_y, z and v_z in 1995.4. The inclination angles of the orbit's plane, $\theta = \arccos\left(L_z/|\vec{L}|\right)$, with $\vec{L} = m\vec{r} \times \dot{\vec{r}}$, are shown next to the orbits. The minimal inclination angle that describes the data in the black hole case is $\theta = 70^o$, while in the fermion ball scenario it is $\theta = 0^o$. In the black hole case, the minimal and maximal distances from Sgr A* are $r_{\rm min} = 0.25''$ and $r_{\rm max} = 0.77''$, respectively, for the orbit with $z = 0.25''$ and $v_z = 0$ which has a period of $T_0 \approx 161$ yr. The orbits with $z = 0.25''$ and $v_z = 400$ km s^{-1} or $z = 0.25''$ and $v_z = 700$ km s^{-1} have periods of $T_0 \approx 268$ yr or $T_0 \approx 3291$ yr, respectively. In the fermion ball scenario, the open orbit with $z = 0.1''$ and $v_z = 0$ has a "period" of $T_0 \approx 77$ yr with $r_{\rm min} = 0.13''$ and $r_{\rm max} = 0.56''$. The open orbits with $z = 0.1''$ and $v_z = 400$ km s^{-1} or $z = 0.1''$ and $v_z = 900$ km s^{-1} have "periods" of $T_0 \approx 100$ yr or $T_0 \approx 1436$ yr, respectively.

In concluding, it is important to note that, based on the data of the star S0-1 [12], the fermion ball scenario cannot be ruled out. In fact, in view of the $z - v_z$ phase space, that is much larger in the fermion ball scenario than in the black hole case, there is reason to treat the fermion ball scenario of the supermassive compact dark object at the center of our Galaxy with the respect it deserves.

3 Dark Matter in the Center and the Halo of the Galaxy

Degenerate fermion balls are well understood in terms of the Thomas-Fermi theory applied to self-gravitating fermionic matter at $T = 0$ [3]. Extending this theory to nonzero temperature [22, 23, 24], it has been shown that at some critical temperature $T = T_{\rm c}$, a self-gravitating ideal fermion gas, having a mass below the OV limit enclosed in a spherical cavity of radius R, may undergo a first-order gravitational phase transition from a diffuse state to a condensed state. This is best seen plotting the energy and free energy as functions of the temperature which are three-valued in some temperature interval, exhibiting a Maxwell-Boltzmann branch at high temperatures and the degenerate branch at low temperatures. However, this first-order phase transition can only take place if the Fermi gas is able to get rid of the large latent heat which is due to the binding energy of the fermion ball. As the short-range interactions of the fermions are negligible, the gas cannot release its latent heat; it will thus be trapped for temperatures $T < T_{\rm c}$ in a thermodynamic quasi-stable supercooled state close to the point of gravothermal collapse. The Fermi gas will be caught in the supercooled state even if the total mass of the gas exceeds the OV limit, as a stable condensed state does not exist in this case.

The formation of a supercooled state close to the point of gravothermal collapse, may be understood as a process similar to that of violent relaxation, which was introduced to describe rapid virialization of stars of different mass in globular clusters [25, 26] without invoking binary collisions of the stars, as these would not contribute significantly to thermalization on a scale of the age of the Universe. Through the gravitational collapse of a cold overdense fluctuation, ~ 1 Gyr after the Big Bang, part of gravitational energy transforms into the kinetic energy of random motion of small-scale density fluctuations. The resulting virialized cloud will thus be well approximated by a gravitationally stable thermalized halo. In order to estimate the mass-temperature ratio, we assume that the cold overdense cloud of the mass of the Galaxy M stops expanding at the time $t_{\rm m}$, reaching its maximal radius $R_{\rm m}$ and minimal average density $\rho_{\rm m} = 3M/(4\pi R_{\rm m}^3)$. The total energy per particle is just the gravitational energy

$$E = -\frac{3}{5}\frac{GM}{R_{\rm m}}\,. \tag{1}$$

Assuming spherical collapse [27] one arrives at

$$\rho_{\rm m} = \frac{9\pi^2}{16}\bar{\rho}(t_{\rm m}) = \frac{9\pi^2}{16}\Omega_{\rm d}\rho_0(1+z_{\rm m})^3, \tag{2}$$

where $\bar{\rho}(t_{\rm m})$ is the background density at the time $t_{\rm m}$ or cosmological redshift $z_{\rm m}$, and $\rho_0 \equiv 3H_0^2/(8\pi G)$ is the present critical density. We now approximate the virialized cloud by a singular isothermal sphere [26] of mass M and radius R, characterized by a constant

circular velocity $\Theta = (2T/m)^{1/2}$ and the density profile $\rho(r) = \Theta^2/4\pi G r^2$. Its total energy per particle is the sum of gravitational and thermal energies, i.e.,

$$E = -\frac{1}{4}\frac{GM}{R} = -\frac{1}{4}\Theta^2. \tag{3}$$

Combining Eqs. (1), (2), and (3), we find

$$\Theta^2 = \frac{6\pi}{5} G (6\Omega_{\rm d}\rho_0 M^2)^{1/3}(1+z_{\rm m}). \tag{4}$$

Taking $\Omega_{\rm d} = 0.3$, $M = 2\times 10^{12} M_\odot$, $z_{\rm m} = 4$, and $H_0 = 65\,{\rm km\,s^{-1}Mpc^{-1}}$, we find $\Theta \simeq 220\,{\rm km\,s^{-1}}$, which corresponds to the mass-temperature ratio $m/T \simeq 4\times 10^6$.

Next, we briefly discuss the general-relativistic extension of the Thomas-Fermi theory [23] for a self-gravitating gas of N fermions with mass m and degeneracy factor g at the temperature T enclosed in a sphere of radius R. We denote by p, ρ, and n the pressure, energy density, and particle number density of the gas, respectively. In the following we use the units in which $G = 1$. The metric generated by the mass distribution is static, spherically symmetric, and asymptotically flat, i.e.,

$$ds^2 = \xi^2 dt^2 - (1-2\mathcal{M}/r)^{-1}dr^2 - r^2(d\theta^2 + \sin\theta d\phi^2). \tag{5}$$

For numerical convenience, we introduce the parameter $\alpha = \mu/T$ and the substitution $\xi = (\varphi+1)^{-1/2}\mu/m$, where μ is the chemical potential associated with the conserved particle number N. The equation of state for a self-gravitating gas may thus be represented in parametric form [28] as

$$n = \frac{1}{\pi^2}\int_0^\infty dy \frac{y^2}{1+\exp\{[(y^2+1)^{1/2}/(\varphi+1)^{1/2}-1]\alpha\}}, \tag{6}$$

$$\rho = \frac{1}{\pi^2}\int_0^\infty dy \frac{y^2(y^2+1)^{1/2}}{1+\exp\{[(y^2+1)^{1/2}/(\varphi+1)^{1/2}-1]\alpha\}}, \tag{7}$$

$$p = \frac{1}{3\pi^2}\int_0^\infty dy \frac{y^4(y^2+1)^{-1/2}}{1+\exp\{[(y^2+1)^{1/2}/(\varphi+1)^{1/2}-1]\alpha\}}, \tag{8}$$

where appropriate length and mass scales a and b, respectively, have been chosen such that $a = b = (2/g)^{1/2}/m^2$. Restoring $\hbar$, c, and G, we have

$$a = \sqrt{\frac{2}{g}}\frac{\hbar M_{\rm Pl}}{cm^2} = 1.0798\times 10^{10}\sqrt{\frac{2}{g}}\left(\frac{15{\rm keV}}{m}\right)^2 {\rm km}, \tag{9}$$

$$b = \sqrt{\frac{2}{g}}\frac{M_{\rm Pl}^3}{m^2} = 0.7251\times 10^{10}\sqrt{\frac{2}{g}}\left(\frac{15{\rm keV}}{m}\right)^2 M_\odot\,. \tag{10}$$

Thus fermion mass, degeneracy factor, and chemical potential are eliminated from the equation of state.

Einstein's field equations for the metric (5) are given by

$$\frac{d\varphi}{dr} = -2(\varphi+1)\frac{\mathcal{M}+4\pi r^3 p}{r(r-2\mathcal{M})}\,, \tag{11}$$

$$\frac{d\mathcal{M}}{dr} = 4\pi r^2 \rho. \tag{12}$$

To these two equations we add

$$\frac{d\mathcal{N}}{dr} = 4\pi r^2 (1-2\mathcal{M}/r)^{-1/2} n \tag{13}$$

imposing particle-number conservation as a condition at the boundary

$$\mathcal{N}(R) = N. \tag{14}$$

Eqs. (11)-(13) should be integrated using the boundary conditions at the origin, i.e.,

$$\varphi(0) = \varphi_0 > -1\,, \qquad \mathcal{M}(0) = 0\,, \qquad \mathcal{N}(0) = 0. \tag{15}$$

It is useful to introduce the degeneracy parameter $\eta = \alpha\varphi/2$, which, in the Newtonian limit, approaches $\eta_{\rm nr} = (\mu_{\rm nr} - V)/T$, with $\mu_{\rm nr} = \mu - m$ being the nonrelativistic chemical potential and V the Newtonian potential. As φ is monotonously decreasing with increasing r, the strongest degeneracy is obtained at the center with $\eta_0 = \alpha\varphi_0/2$. The parameter η_0, uniquely related to the central density and pressure, will eventually be fixed by the requirement (14). For $r \geq R$, the function φ yields the usual empty-space Schwarzschild solution

$$\varphi(r) = \frac{\mu^2}{m^2}\left(1 - \frac{2M}{r}\right)^{-1} - 1\,, \tag{16}$$

with

$$M = \mathcal{M}(R) = \int_0^R dr 4\pi r^2 \rho(r). \tag{17}$$

Given the temperature T, the set of self-consistency equations (6)-(13), with the boundary conditions (14)-(17) defines the general-relativistic extension of the Thomas-Fermi equation.

4 Numerical Results

The numerical procedure is now straightforward. For a fixed, arbitrarily chosen α, we first integrate Eqs. (11) and (12) numerically on the interval $[0, R]$ to find the solutions for various central values of the degeneracy parameter η_0. Integrating (13) simultaneously,

yields $\mathcal{N}(R)$ as a function of η_0. We then select the value of η_0 for which $\mathcal{N}(R) = N$. The chemical potential μ corresponding to this particular solution is given by Eq. (16) which in turn yields the parametric dependence on the temperature through $\alpha = \mu/T$.

The quantities N, T,and R are free parameters of our model and their range of values are dictated by the physics of the problem at hand. At $T = 0$ the number of fermions N is restricted by the OV limit $N_{\rm OV} = 2.89 \times 10^9 \sqrt{2/g}(15\,{\rm keV}/m)^2 M_\odot/m$. However, at nonzero temperature, stable solutions exist with $N > N_{\rm OV}$, depending on temperature and radius. In the following N is required to be of the order $2\times 10^{12} M_\odot/m$, so that for any m, the total mass is close to the estimated mass of the halo [30]. As we have demonstrated, the expected particle mass-temperature ratio of the halo is given by $\alpha \simeq m/T = 4 \times 10^4$. The halo radius R is in principle unlimited; in practice, however, it should not exceed half the average intergalactic distance. It is known that an isothermal configuration has no natural boundary, in contrast to the degenerate case of zero temperature, where for given N (up to the OV limit) the radius R is naturally fixed by the condition of vanishing pressure and density. At nonzero temperature, with R being unbounded, our gas would occupy the entire space, and fixing N would make p and ρ vanish everywhere. Conversely, if we do not fix N and integrate the equations on the interval $[0, \infty)$, both M and N will diverge at infinity for $T > 0$. Thus, one is forced to introduce a cutoff. In an isothermal model of a similar kind [35], the cutoff was set at the radius R, where the energy density was by about six orders of magnitude smaller than the central value. Our choice of $R = 200$ kpc is based on the estimated size of the Galactic halo.

The only remaining free parameters of our model are the fermion mass m and the degeneracy factor g, which always appear in the combination $m^4 g$. We fix these parameters at $m = 15$ keV and $g = 2$, and justify this choice *a posteriori*.

The results of numerical integration of Eqs. (11) and (12), without restricting N, are presented in Fig. 5, where we plot the particle number N as a function of the central degeneracy parameter η_0 for several values of α close to 4×10^6. For fixed N, there is a range of α, where the Thomas-Fermi equation has multiple solutions. For example, for $N = 2 \times 10^{12}$ and $\alpha = 4 \times 10^6$ six solutions are found, which are denoted by (1), (2), (3), (3'), (2'), and (1') corresponding to the values η_0 = -30.528, -25.354, -22.390, 29.284, 33.380, and 40.479, respectively. In Figs. 6 and 7 we plot the corresponding density profiles and enclosed masses, respectively. For negative central value η_0, for which the degeneracy parameter is negative everywhere, the system behaves basically as a Maxwell-Boltzmann isothermal sphere. Positive values of the central degeneracy parameter η_0 are characterized by a pronounced central core of mass of about $2.5 \times 10^6 M_\odot$ within a radius of about 20 mpc. The presence of this core is obviously due to the degeneracy pressure of the Fermi-Dirac statistics. A similar structure was obtained in collisionless stellar systems modeled as a nonrelativistic Fermi gas [29].

Figs. 6 and 7 show two important features. First, a galactic halo at a given temperature T may or may not have a central core depending whether the central degeneracy parameter η_0 is positive or negative. Second, the closer to zero η_0 is, the smaller the

radius is at which the r^{-2} asymptotic behavior of the density begins. The flattening of the Galactic rotation curve begins in the range $1 \lesssim r/\mathrm{kpc} \lesssim 10$, hence the solution (3') most likely describes the Galaxy's halo. This may be verified by calculating the rotational curves in our model. We know already from the estimate (4) that our model yields the correct asymptotic circular velocity of 220 km/s. In order to make a more realistic comparison with the observed Galactic rotation curve, we must include two additional matter components: the bulge and the disk. The bulge is modeled as a spherically symmetric matter distribution of the form [31]

$$\rho_{\mathrm{b}}(s) = \frac{e^{-hs}}{2s^3} \int_0^\infty du \frac{e^{-hsu}}{[(u+1)^8 - 1]^{1/2}}\,, \tag{18}$$

where $s = (r/r_0)^1/4$, r_0 is the effective radius of the bulge and h is a parameter. We adopt $r_0 = 2.67$ kpc and h yielding the bulge mass $M_{\mathrm{b}} = 1.5 \times 10^{10} M_\odot$ [32]. In Fig. 8 the mass of halo and bulge enclosed within a given radius is plotted for various η_0. Here, the gravitational backreaction of the bulge on the fermionic halo has been taken into account. The data points, indicated by squares, are the mass $M_{\mathrm{c}} = 2.6 \times 10^6 M_\odot$ within 18 mpc, estimated from the motion of the stars near Sgr A* [12], and the mass $M_{50} = 5.4^{+0.2}_{-3.6} \times 10^{11}$ within 50 kpc, estimated from the motions of satellite galaxies and globular clusters [30]. Variation of the central degeneracy parameter η_0 between 24 and 32 does not change the essential halo features.

In Fig. 9 we plot the circular velocity components of the halo, the bulge, and the disk. The contribution of the disk is modeled as [33]

$$\Theta_{\mathrm{d}}(r)^2 = \Theta_{\mathrm{d}}(r_{\mathrm{o}})^2 \frac{1.97(r/r_{\mathrm{o}})^{1.22}}{[(r/r_{\mathrm{o}})^2 + 0.78^2]^{1.43}}\,, \tag{19}$$

where we take $r_{\mathrm{o}} = 13.5$ kpc and $\Theta_{\mathrm{d}} = 100$ km/s. Here it is assumed for simplicity that the disk does not influence the mass distribution of the bulge and the halo. Choosing the central degeneracy $\eta_0 = 28$ for the halo, the data by Merrifield and Olling [34] are reasonably well fitted.

We now turn to the discussion of our choice of the fermion mass $m = 15$ keV for a degeneracy factor $g = 2$. To this end we investigate how the mass of the central object, i.e., the mass M_{c} within 18 mpc, depends on m in the interval 5 to 25 keV, for various η_0. We find that $m \simeq 15$ keV gives always the maximal value of M_{c} ranging between 1.7 to $2.3 \times 10^6 M_\odot$ for η_0 between 20 and 28. Hence, with $m \simeq 15$ keV we get the value closest to the mass of the central object M_{c} estimated from the motion of the stars near Sgr A* [12].

We now present the results of the calculations for fixed particle number and temperatures near the point of gravothermal collapse. In Fig. 10 the energy per particle defined as $E = M/N - m$ is plotted as a function of temperature for fixed $N = 2 \times 10^{12}$. The plot looks very much like that of a canonical Maxwell-Boltzmann ensemble [26], with

one important difference: in the Maxwell-Boltzmann case the curve continues to spiral inwards *ad infinitum* approaching the point of the singular isothermal sphere, that is characterized by an infinite central density. In Fermi-Dirac case the spiral consists of two almost identical curves. The inwards winding of the spiral begins for some negative central degeneracy and stops at the point $T = 2.3923 \times 10^{-7}m$, $E = -1.1964 \times 10^{-7}m$, where η_0 becomes zero. This part of the curve, which basically depicts the behavior of a nondegenerate gas, we call *Maxwell-Boltzmann branch*. By increasing the central degeneracy parameter further to positive values, the spiral begins to unwind outwards very close to the inwards winding curve. The outwards winding curve will eventually depart from the Maxwell-Boltzmann branch for temperatures $T \gtrsim 10^{-3}m$. Further increase of the central degeneracy parameter brings us to a region, where general-relativistic effects become important. The curve will exhibit another spiral for temperatures and energies of the order of a few $10^{-3}m$ approaching the limiting temperature $T_\infty = 2.4 \times 10^{-3}m$ and energy $E_\infty = 3.6 \times 10^{-3}m$ with both the central degeneracy parameter and the central density approaching infinite values. It is remarkable that gravitationally stable configurations with arbitrary large central degeneracy parameters exist at finite temperature even though the total mass exceeds the OV limit by several orders of magnitude.

5 Conclusions

In summary, using the Thomas-Fermi theory, we have shown that a weakly interacting fermionic gas at finite temperature yields a mass distribution that successfully describes both the center and the halo of the Galaxy. For a fermion mass $m \simeq 15$ keV, a reasonable fit to the rotation curve is achieved with the temperature $T = 3.75$ meV and the degeneracy parameter at the center $\eta_0 = 28$. With the same parameters, we obtain the mass $M_{50} = 5.04 \times 10^{11} M_\odot$ and $M_{200} = 2.04 \times 10^{12} M_\odot$ within 50 and 200 kpc, respectively. These values agree quite well with the mass estimates based on the motions of satellite galaxies and globular clusters [30]. Moreover, the mass of $M_c \simeq 2.27 \times 10^6 M_\odot$, enclosed within 18 mpc, agrees reasonably well with the observations of the compact dark object at the center of the Galaxy. We thus conclude that both the Galactic halo and center could be made of the same fermions.

An observational consequence of this unified scenario of fermion ball and fermion halo at finite temperature could be the direct observation of the radiative decay of the fermion (assumed here to be a sterile neutrino) into a standard neutrino, i.e., $f \to \nu\gamma$. The X-ray luminosity of the compact dark object is most easily observed. If the lifetime for the decay $f \to \nu\gamma$ is 0.82 $\times 10^{19}$ yr, the luminosity of a $M_c = 2.6 \times 10^6 M_\odot$ fermion ball would be 0.9 $\times 10^{34}$ erg s^{-1}. This is consistent with the upper limit of the X-ray luminosity of $\sim$ (0.5 - 0.9) $\times 10^{34}$ erg s^{-1} of the source with radius $0.5'' \simeq 23$ light-days, whose center nearly coincides with Sgr A*, as seen by the Chandra satellite in the 2 to 7 keV band [36]. The lifetime is proportional to $\sin^{-2}\theta$, θ being the unknown mixing angle of the sterile with active neutrinos. With a lifetime of 0.82×10^{19} yr we obtain an acceptable value for the

mixing angle squared of $\theta^2 = 1.4 \times 10^{-11}$. The X-rays originating from such a radiative decay would contribute about two orders of magnitude less than the observed diffuse X-ray background at this wavelength if the sterile neutrino is the dark matter particle of the Universe. The signal observed at the Galactic center would be a sharp X-ray line at ~ 7.5 keV for $g = 2$ and ~ 6.3 keV for $g = 4$. This line could be misinterpreted as the Fe K_α line at 6.67 keV. Scattering with baryonic matter within the Galactic center could distribute the energy more evenly in the 2 to 7 keV band. The X-ray luminosity would be tracing the fermion matter distribution, and it could thus be an important test of the fermion ball scenario. Of course the angular resolution would need to be $\lesssim 0.1''$ and the sensitivity would have to extend beyond 7 keV.

ACKNOWLEDGEMENTS

This research is in part supported by the Foundation of Fundamental Research (FFR) grant number PHY99-01241 and the Research Committee of the University of Cape Town. The work of N.B. is supported in part by the Ministry of Science and Technology of the Republic of Croatia under Contract No. 00980102.

References

[1] M.A. Markov, Phys. Lett. **10**, 122 (1964).

[2] G. Marx and A.S. Szalay, in *Neutrino '72*, **1**, 191 (Technoinform, Budapest, 1972); R. Cowsik and J. McClelland, Astrophys. J. **180**, 7 (1973); R. Ruffini, Lett. Nuovo Cim. **29**, 161 (1980).

[3] R.D. Viollier, D. Trautmann and G.B. Tupper, Phys. Lett. B **306**, 79 (1993); R.D. Viollier, Prog. Part. Nucl. Phys. **32**, 51 (1994).

[4] N. Bilić, D. Tsiklauri and R.D. Viollier, Prog. Part. Nucl. Phys. **40**, 17 (1998); N. Bilić and R.D. Viollier, Nucl. Phys. (Proc. Suppl.) B **66**, 256 (1998).

[5] N. Bilić, F. Munyaneza and R.D. Viollier, Phys. Rev. D **59**, 024003 (1999).

[6] D. Tsiklauri and R.D. Viollier, Astropart. Phys. **12**, 199 (1999); F. Munyaneza and R.D. Viollier, astro-ph/9907318.

[7] F. Munyaneza, D. Tsiklauri and R.D. Viollier, Astrophys. J. **509**, L105 (1998); *ibid.* **526**, 744 (1999); F. Munyaneza and R.D. Viollier, astro-ph/0103466, Astrophys. J. **563**, 0000 (2001).

[8] L.C. Ho and J. Kormendy, astro-ph/0003267; astro-ph/0003268.

[9] P. Bode, J.P. Ostriker, and N. Turok, Astrophys. J. **556**, 93 (2001), astro-ph/0010389.

[10] F. Macchetto *et al.*, Astrophys. J. **489**, 579 (1997).

[11] J.R. Oppenheimer and G.M. Volkoff, Phys. Rev. **55**, 374 (1939).

[12] A. Eckart and R. Genzel, Mon. Not. R. Astron. Soc. **284**, 576 (1997); A.M. Ghez, B.L. Klein, M. Morris and E.E. Becklin, Astrophys. J. **509**, 678 (1998).

[13] R. Mahadevan, Nature **394**, 651 (1998).

[14] E.W. Kolb and M.S. Turner, *The Early Universe* (Addison-Wesley, San Francisco, 1989).

[15] S. Fukuda *et al.*, Phys. Rev. Lett. **85**, 3999 (2000).

[16] D. E. Groom *et al.*, *Review of Particle Physics*, Eur. Phys. J. C **15**, 1 (2000).

[17] X. Shi and G.M. Fuller, Phys. Rev. Lett. **82**, 2832 (1999); K. Abazajian, G.M. Fuller, and M. Patel, Phys. Rev. D **64**, 023501 (2001), astro-ph/0101524; G.B. Tupper, R.J. Lindebaum, and R.D. Viollier, Mod. Phys. Lett. A 15, 1221 (2000).

[18] T. Goto and M. Yamaguchi, Phys. Lett. B **276**, 123 (1992); L. Covi , J.E. Kim, and L. Roszkowski, Phys. Rev. Lett. **82**, 4180 (1999), hep-ph/9905212; L. Covi , H.-B. Kim, J.E. Kim, and L. Roszkowski, hep-ph/0101009.

[19] M. Dine and A.E. Nelson, Phys. Rev. D **48**, 1277 (1993), hep-ph/9303230; M. Dine, A.E. Nelson and Y. Shirman, Phys. Rev. D **51**, 1362 (1995), hep-ph/9408384; M. Dine, A.E. Nelson, Y. Nir and Y. Shirman, Phys. Rev. D **53**, 2658 (1996), hep-ph/9507378; D.H. Lyth, Phys. Lett. B **488**, 417 (2000), hep-ph/9911257.

[20] H. Murayama, Phys. Rev. Lett. **79**, 18 (1997), hep-ph/9705271; S. Dimopoulos, G. Dvali, R. Rattazzi and G.F. Giudice, Nucl. Phys. B **510**, 12 (1998), hep-ph/9705307; E.A. Baltz and H. Murayama, astro-ph/0108172.

[21] S. Cole and C. Lacey, Mon. Not. R. Astron. Soc. **281**, 716 (1996) and references therein.

[22] N. Bilić and R.D. Viollier, Phys. Lett. B **408**, 75 (1997).

[23] N. Bilić and R.D. Viollier, Gen. Rel. Grav. **31**, 1105 (1999); Eur. Phys. J. B **11**, 173 (1999).

[24] W. Thirring, Z. Physik **235**, 339 (1970); P. Hertel, H. Narnhofer and W. Thirring, Comm. Math. Phys. **28**, 159 (1972); J. Messer, J. Math. Phys. **22**, 2910 (1981).

[25] D. Lynden-Bell, Mon. Not. R. Astron. Soc. **136**, 101 (1967).

[26] J. Binney and S. Tremaine, *Galactic Dynamics* (Princeton University Press, Princeton, New Jersey, 1987), and references cited therein.

[27] T. Padmanabhan, *Structure formation in the Universe* (Cambridge University Press, Cambridge, 1993).

[28] J. Ehlers, in *Relativity, Astrophysics and Cosmology*, edited by W. Israel (D. Reidel Publishing Company, Dordrecht/Boston 1973).

[29] P.-H. Chavanis and J. Sommeria, Mon. Not. R. Astron. Soc. **296**, 569 (1998).

[30] M.I. Wilkinson and N.W. Evans, Mon. Not. R. Astron. Soc. **310**, 645 (1999).

[31] P.J. Young, Astrophys. J. **81**, 807 (1976); G. de Vaucouleurs and W.D. Pence, Astrophys. J. **83**, 1163 (1978).

[32] P.D. Sackett, Astrophys. J. **483**, 103 (1997).

[33] M. Persic, P. Salucci, and F. Stell, Mon. Not. R. Astron. Soc. **281**, 27 (1986).

[34] R.P. Olling and M.R. Merrifield, Mon. Not. R. Astron. Soc. **311**, 361 (2000).

[35] W.Y. Chau, K. Lake, J. Stone, Astrophys. J. **281**, 560 (1984).

[36] F.K. Baganoff *et al.*, astro-ph/0102151.

Figure 1: Right ascension of S0-1 versus time for various $|z|$ and $v_x = 340$ km s^{-1}, $v_y = -1190$ km s^{-1} and $v_z = 0$ in 1995.4.

Figure 2: Declination of S0-1 versus time for various $|z|$ and $v_x = 340$ km s^{-1}, $v_y = -1190$ km s^{-1} and $v_z = 0$ in 1995.4.

Figure 3: The $z - v_z$ phase-space that fits the S0-1 data.

Figure 4: Examples of typical orbits of S0-1.

Figure 5: Number of particles versus central degeneracy parameter for $m/T = 4 \times 10^6$ (solid), 3.5×10^6 (short dashs), 4.5×10^6 (long dashs), and 5×10^6 (dot-dashed line).

Figure 6: The density profile of the halo for a central degeneracy parameter $\eta_0 = 0$ (dotted line) and for the six η_0-values discussed in the text. Configurations with negative η_0 ((1)-(3)) are depicted by the dashed and those with positive η_0 ((1')-(3')) by the solid line.

Figure 7: Mass of the halo $M_{\rm h}(r)$ enclosed within a radius r for various central degeneracy parameters η_0 as in Fig. 6.

Figure 8: Enclosed mass of halo plus bulge versus radius for $\eta_0 = 24$ (dashed), 28 (solid), and 32 (dot-dashed line).

Figure 9: Fit to the rotation curve of the Galaxy. The data points are from [34] for $R_0 = 8.5$ kpc and $\Theta_0 = 220$ km/s.

Figure 10: Energy (shifted by $12 \times 10^{-8} m$) versus temperature (shifted by $-24 \times 10^{-8} m$), both in units of $10^{-10} m$, for fixed $N = 2 \times 10^{12} M_\odot / m$

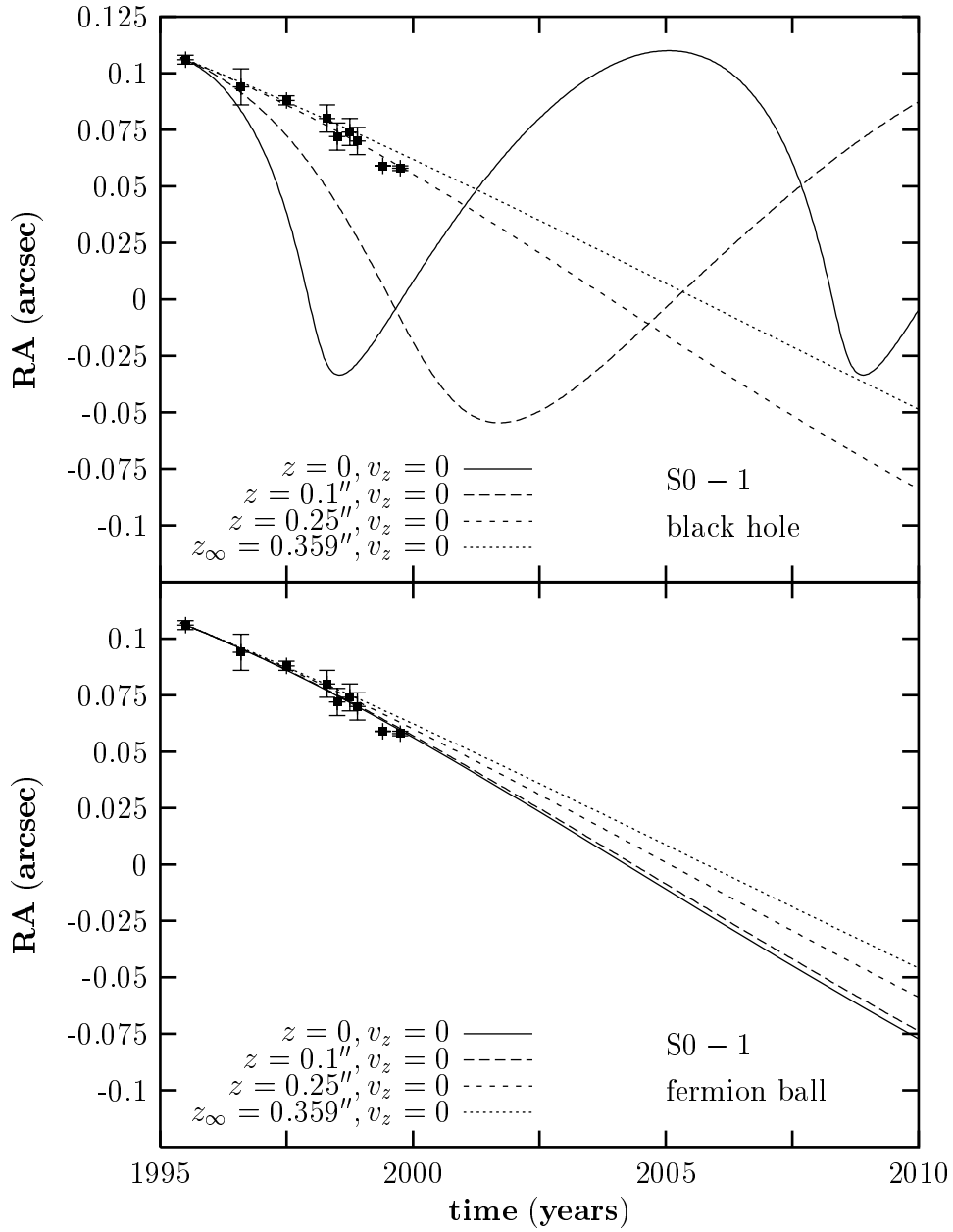
0.125
0.1
0.075
0.05
0.025
0
-0.025
-0.05
-0.075
-0.1
RA (arcsec)
$z = 0, v_z = 0$
$z = 0.1'', v_z = 0$
$z = 0.25'', v_z = 0$
$z_\infty = 0.359'', v_z = 0$
S0 − 1
black hole
S0 − 1
fermion ball
1995
2000
2005
2010
time (years)

Fig.1

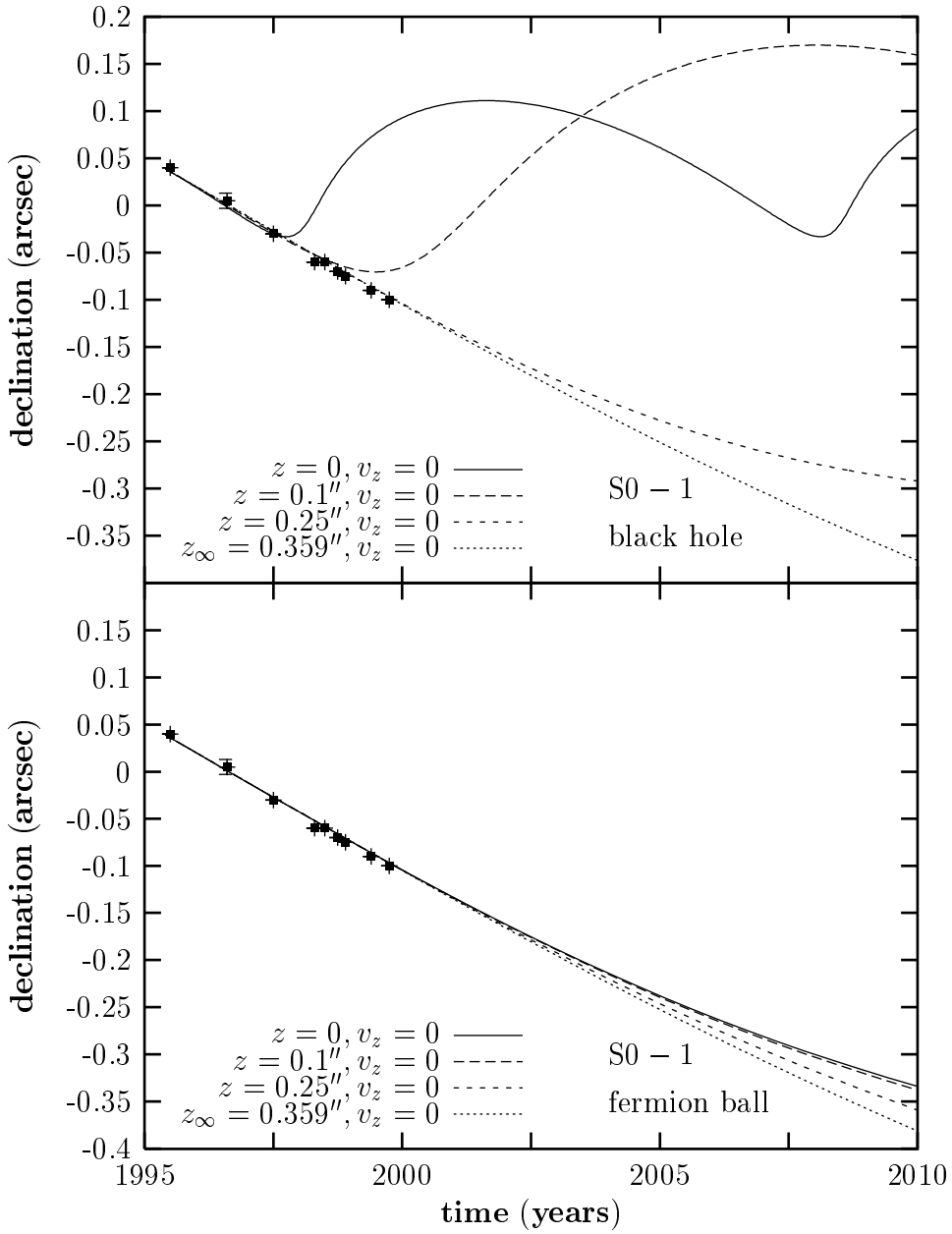
declination (arcsec)
0.2
0.15
0.1
0.05
0
-0.05
-0.1
-0.15
-0.2
-0.25
-0.3
-0.35
$z = 0, v_z = 0$
$z = 0.1'', v_z = 0$
$z = 0.25'', v_z = 0$
$z_\infty = 0.359'', v_z = 0$
S0 − 1
black hole
declination (arcsec)
0.15
0.1
0.05
0
-0.05
-0.1
-0.15
-0.2
-0.25
-0.3
-0.35
-0.4
$z = 0, v_z = 0$
$z = 0.1'', v_z = 0$
$z = 0.25'', v_z = 0$
$z_\infty = 0.359'', v_z = 0$
S0 − 1
fermion ball
1995
2000
2005
2010
time (years)

Fig.2

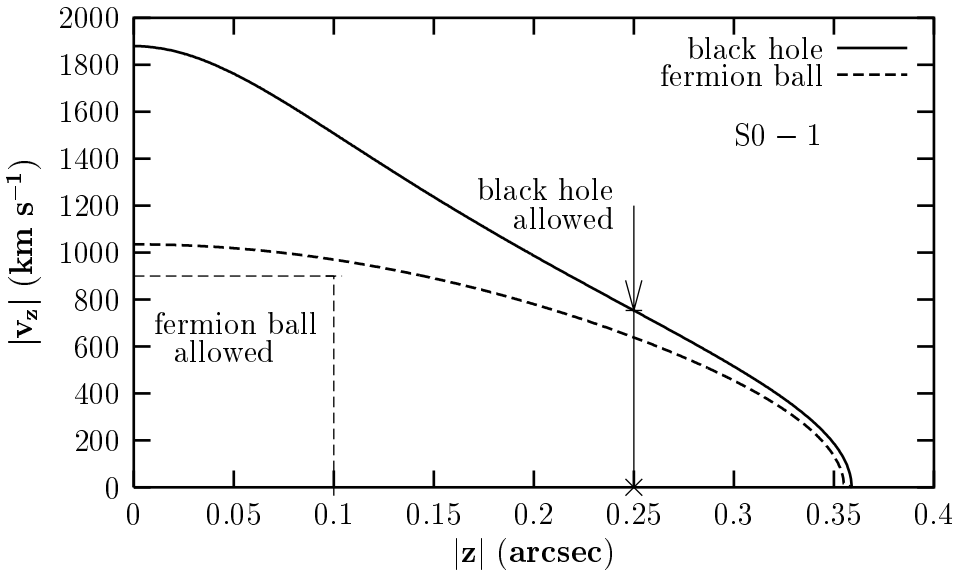
2000
1800
1600
1400
1200
1000
800
600
400
200
0
0
0.05
0.1
0.15
0.2
0.25
0.3
0.35
0.4
black hole
fermion ball
S0 − 1
black hole
allowed
fermion ball
allowed
|vz| (km s−1)
|z| (arcsec)

Fig.3

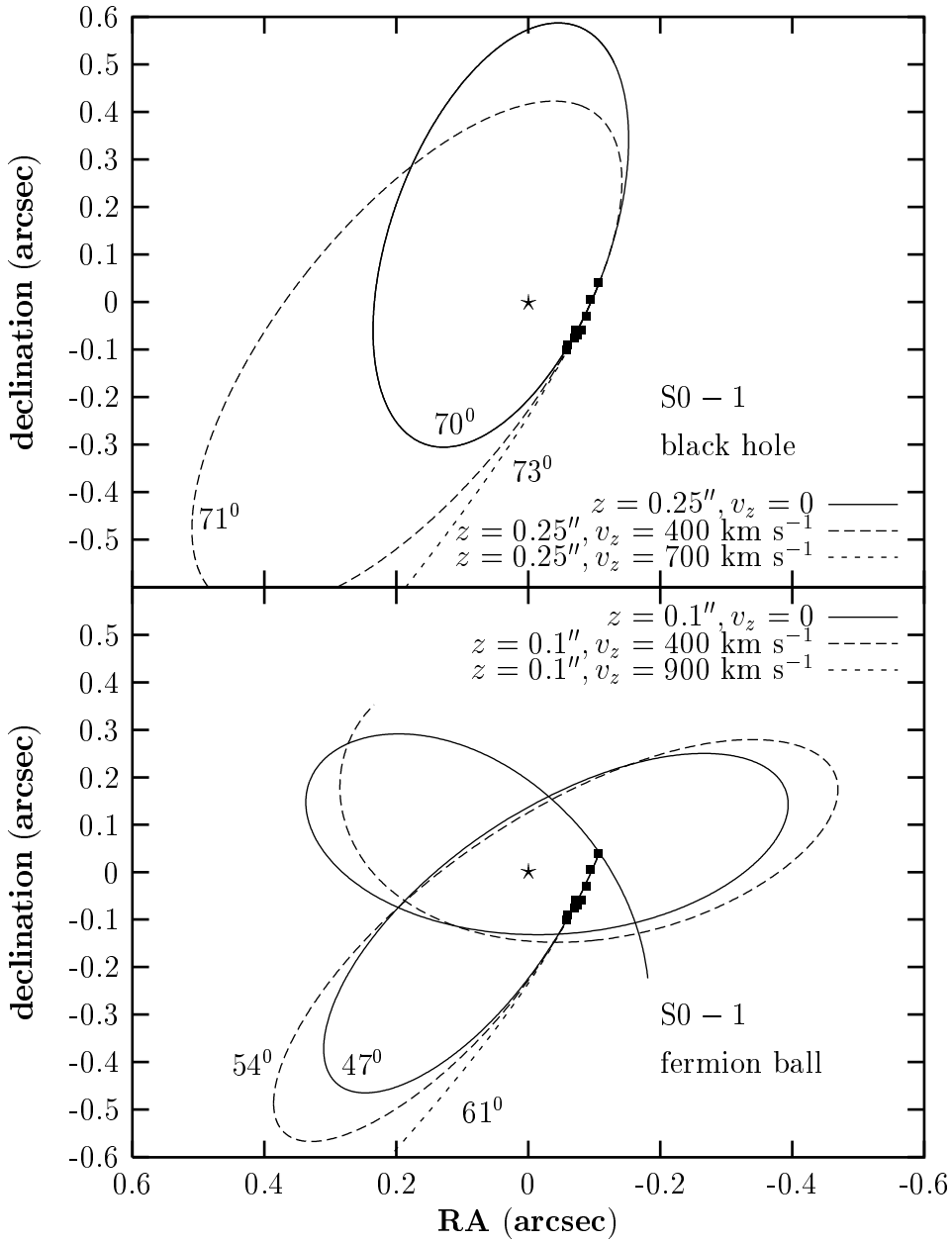
declination (arcsec)
RA (arcsec)
S0 − 1
black hole
$z = 0.25''$, $v_z = 0$
$z = 0.25''$, $v_z = 400$ km s^{-1}
$z = 0.25''$, $v_z = 700$ km s^{-1}
70^0
71^0
73^0
S0 − 1
fermion ball
$z = 0.1''$, $v_z = 0$
$z = 0.1''$, $v_z = 400$ km s^{-1}
$z = 0.1''$, $v_z = 900$ km s^{-1}
47^0
54^0
61^0

Fig.4

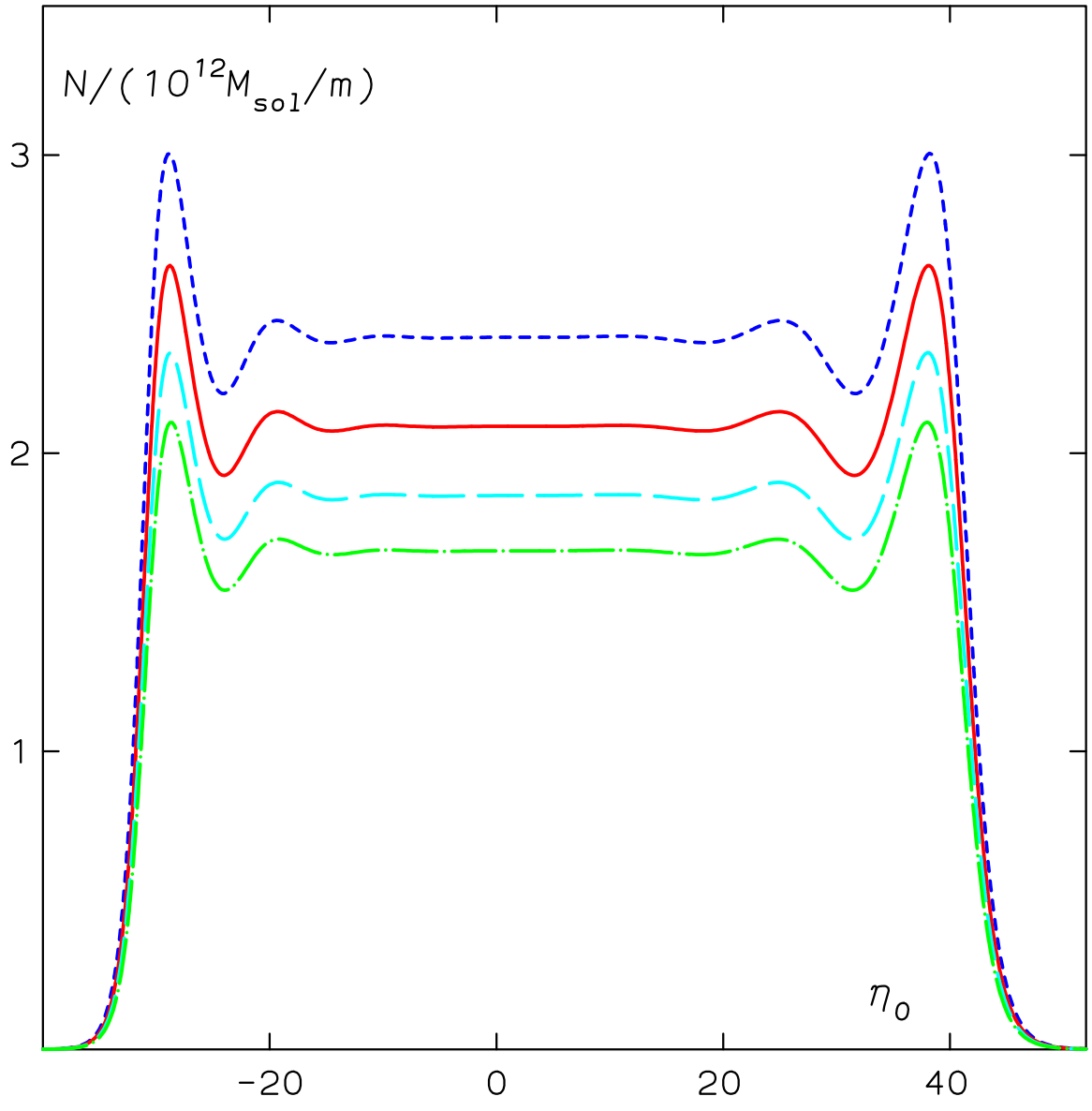

Fig.5

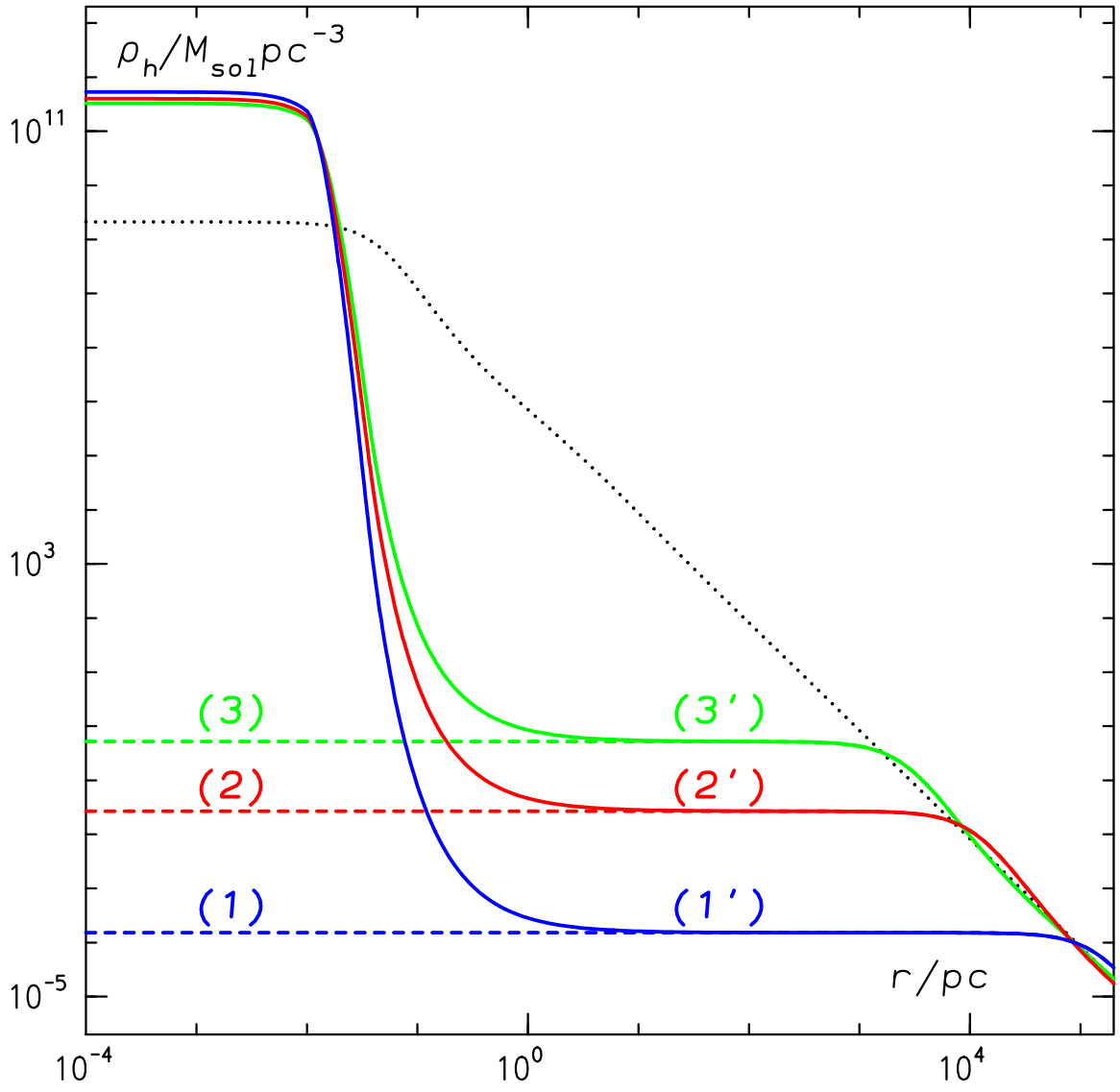

Fig.6

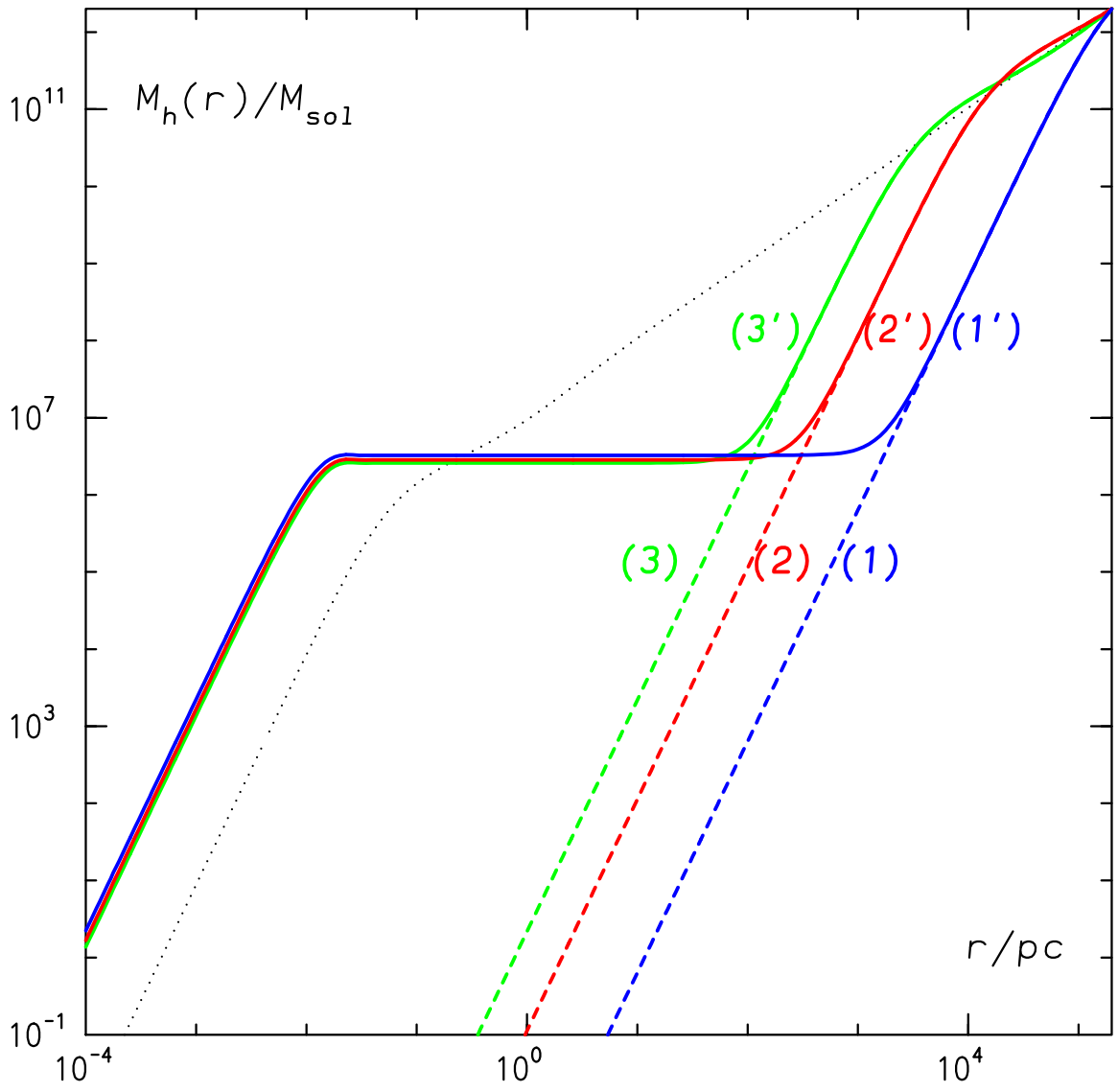

Fig. 7

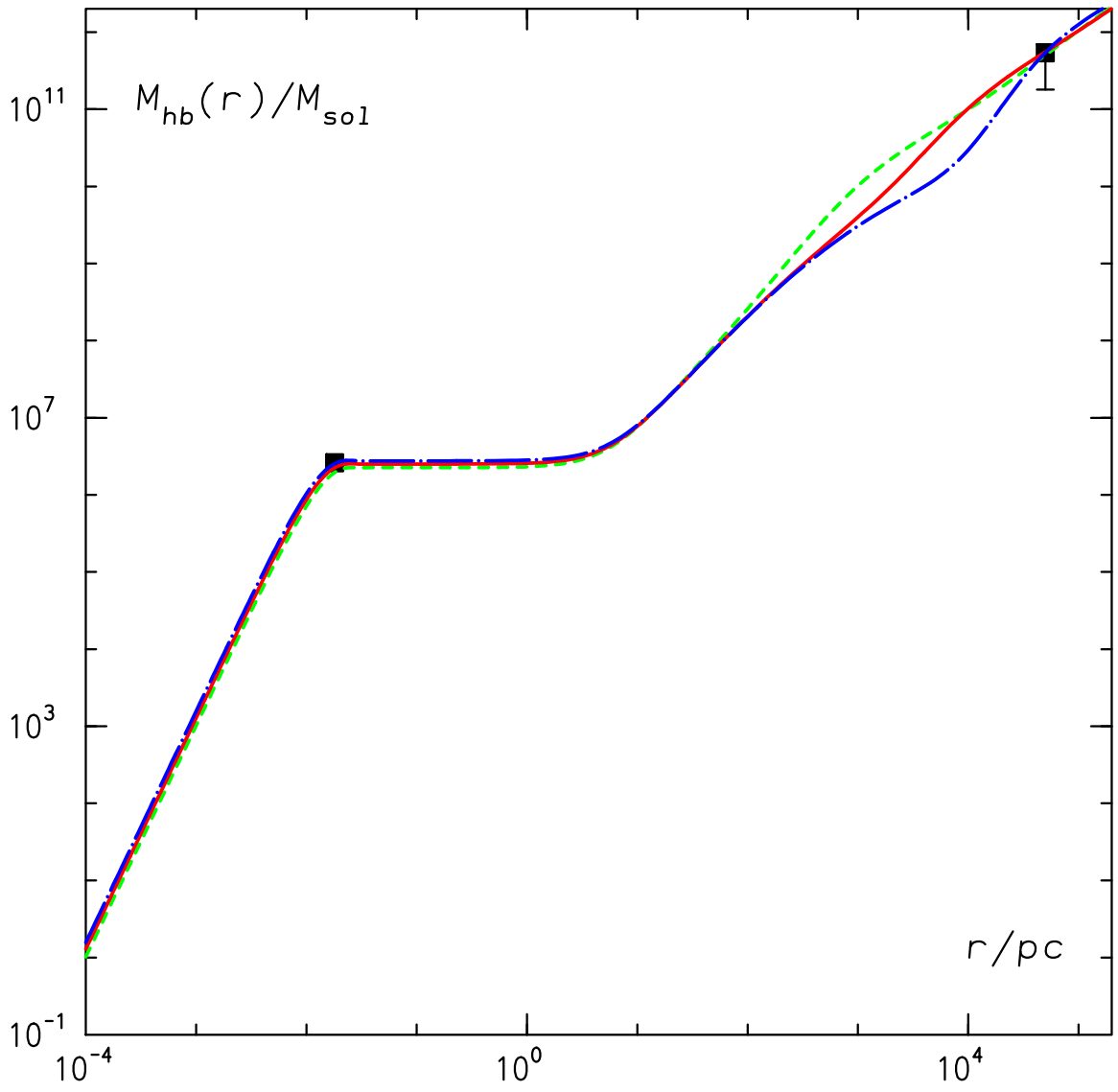

Fig.8

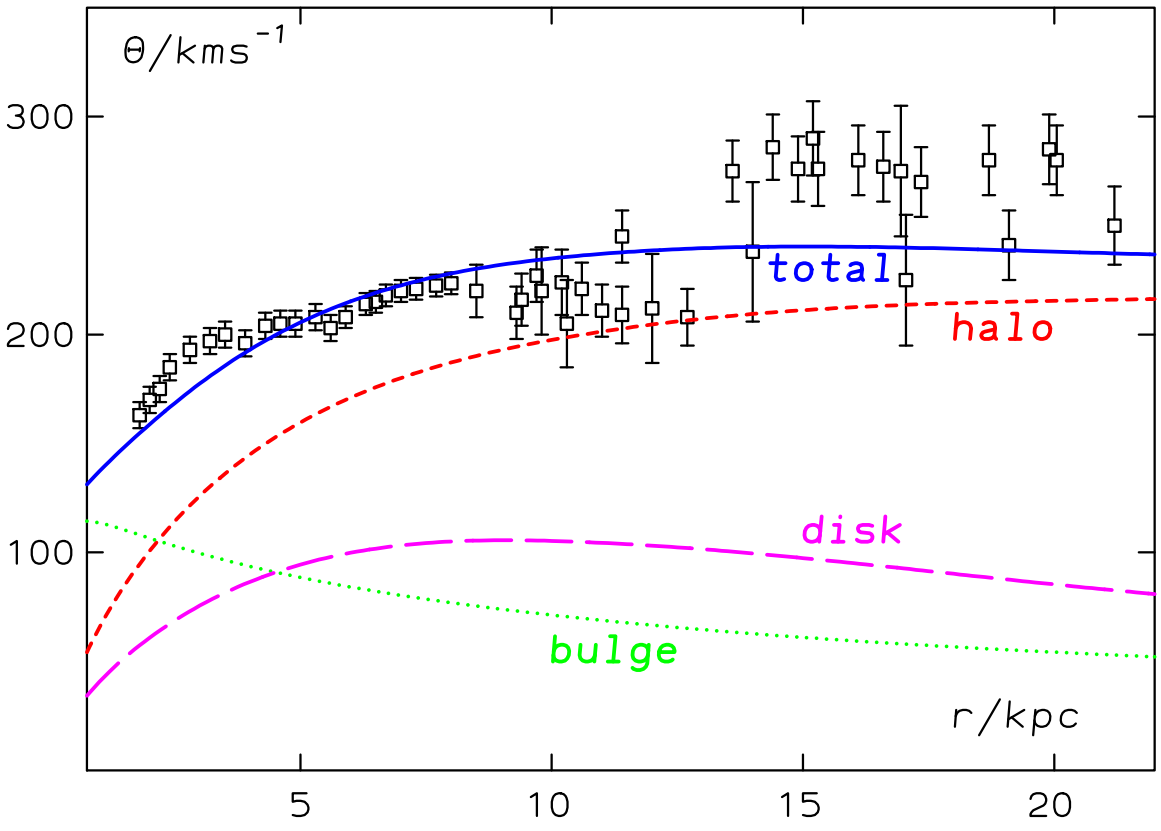

Fig. 9

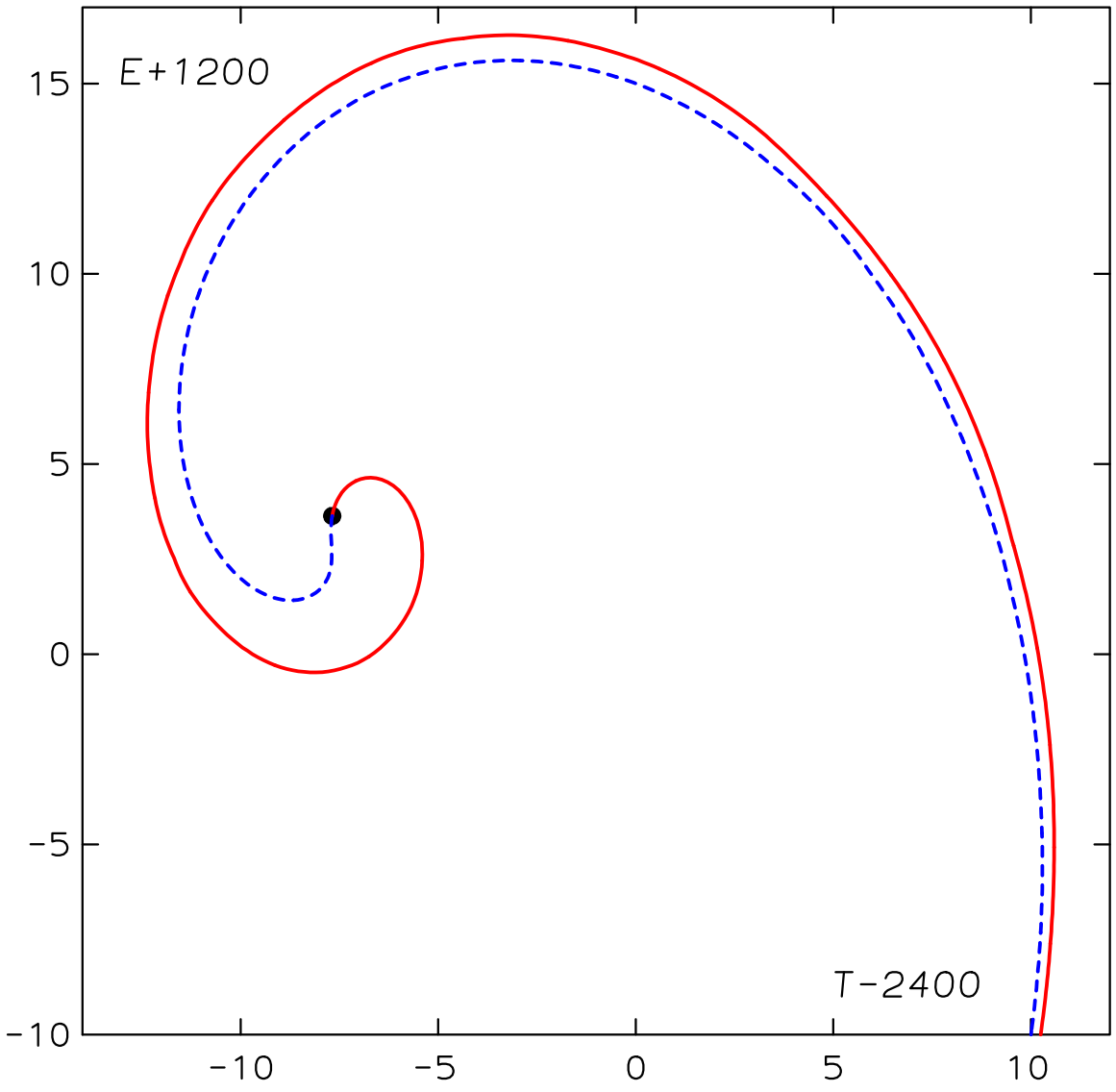

Fig. 10